



THE UNIVERSITY *of* EDINBURGH

Edinburgh Research Explorer

Microbial Host Interactions and Impaired Wound Healing in Mice and Humans: Defining a Role for BD14 and NOD2

Citation for published version:

Williams, H, Campbell, L, Crompton, RA, Singh, G, McHugh, BJ, Davidson, DJ, McBain, AJ, Cruikshank, SM & Hardman, MJ 2018, 'Microbial Host Interactions and Impaired Wound Healing in Mice and Humans: Defining a Role for BD14 and NOD2', *Journal of Investigative Dermatology*, vol. 138, no. 10, pp. 2264-2274. <https://doi.org/10.1016/j.jid.2018.04.014>

Digital Object Identifier (DOI):

[10.1016/j.jid.2018.04.014](https://doi.org/10.1016/j.jid.2018.04.014)

Link:

[Link to publication record in Edinburgh Research Explorer](#)

Document Version:

Peer reviewed version

Published In:

Journal of Investigative Dermatology

General rights

Copyright for the publications made accessible via the Edinburgh Research Explorer is retained by the author(s) and / or other copyright owners and it is a condition of accessing these publications that users recognise and abide by the legal requirements associated with these rights.

Take down policy

The University of Edinburgh has made every reasonable effort to ensure that Edinburgh Research Explorer content complies with UK legislation. If you believe that the public display of this file breaches copyright please contact openaccess@ed.ac.uk providing details, and we will remove access to the work immediately and investigate your claim.



Microbial host interactions and impaired wound healing in mice and humans: defining a role for BD14 and NOD2

Helen Williams¹, Laura Campbell¹, Rachel A. Crompton¹, Gurdeep Singh¹, Brian J. McHugh², Donald J. Davidson², Andrew J. McBain³, Sheena M. Cruickshank^{1*} and Matthew J. Hardman.^{1,4*}

¹ Division of Infection, Immunity & Respiratory Medicine, School of Biological Sciences, Manchester Academic Health Science Centre, ²Medical Research Council Centre for Inflammation Research at the University of Edinburgh, ³Division of Pharmacy and Optometry, School of Health Sciences, Faculty of Biology, Medicine and Health, The University of Manchester, Manchester, M13 9PT, United Kingdom. ⁴ Current address: School of Life Sciences, University of Hull, Cottingham Road, Hull, HU6 7RX, United Kingdom.

* Authors contributed equally to the study

The work was performed in Manchester, United Kingdom

CORRESPONDING AUTHOR: Professor Sheena M. Cruickshank, The University of Manchester, AV Hill Building, Oxford Road, Manchester, M13 9PT, sheena.cruickshank@manchester.ac.uk, Phone +44 (0)161 275 1578

SHORT TITLE: β -defensin 14 and cutaneous wound healing in mice and humans.

ABBREVIATIONS USED: AMP, anti-microbial peptide; DFU, diabetic foot ulcer; DGGE, density gradient gel electrophoresis; hBD, human β -defensin, mBD, murine β -defensin; MDP, muramyl dipeptide; NOD2, nucleotide-binding oligomerisation domain-containing protein 2; PRR, pattern recognition receptor; TLR, Toll-like receptor.

ABSTRACT

Chronic wounds cause significant patient morbidity and mortality. A key factor in their etiology is microbial infection, yet skin host-microbiota interactions during wound repair remain poorly understood. We investigated microbiome profiles of non-infected human chronic wounds and showed that reduced diversity was associated with subsequent healing outcome. Furthermore, poor clinical healing outcome was associated with increased local expression of the pattern recognition receptor *NOD2*. To investigate *NOD2* function in the context of cutaneous healing, we treated mice with the *NOD2* ligand muramyl dipeptide (MDP) and analyzed wound repair parameters and expression of anti-microbial peptides. MDP treatment of littermate controls significantly delayed wound repair associated with reduced re-epithelialization, heightened inflammation and upregulation of murine β -*Defensins* (*mBD*) 1, 3 and particularly 14. We postulated that although BD14 might impact on local skin microbial communities it may further impact other healing parameters. Indeed, exogenously administered mBD14 directly delayed mouse primary keratinocyte scratch wound closure *in vitro*. To further explore the role of mBD14 in wound repair, we employed *Defb14*^{-/-} mice, and showed they had a global delay in healing *in vivo*, associated with alterations in wound microbiota. Taken together these studies suggest a key role for *NOD2*-mediated regulation of local skin microbiota which in turn impacts on chronic wound etiology.

INTRODUCTION

Chronic wounds, which include pressure sores, venous and diabetic foot ulcers (DFUs), are a global problem leading to substantial morbidity and mortality (Gottrup, 2004). Following injury, skin-resident microbiota and pathogenic species may colonise the wound and proliferate (Eming et al., 2014). Hence understanding the role of bacteria, both pathogenic and commensal, in the context of skin wounding is important yet comparatively little research attention has focused on this area (Loesche et al., 2017, Misic et al., 2014).

Poor progression of chronic wounds is often associated with infection and the presence of recalcitrant microbial biofilms comprising *Staphylococcus*, *Pseudomonas* and *Corynebacterium* and a variety of other organisms (Attinger and Wolcott, 2012, James et al., 2008, Mancl et al., 2013, Rhoads et al., 2012). The innate immune system detects infection and injury via pattern recognition receptors (PRRs), such as the Nod-like receptors. PRRs respond to highly conserved microbial structures- pathogen-associated molecular patterns that can trigger inflammatory and defense responses such as keratinocyte-mediated production of anti-microbial peptides (AMPs). AMPs provide rapid and efficient anti-microbial activity against a wide range of pathogens (Dutta and Das, 2016, Harder et al., 2013). The skin has many AMPs including Cathelicidins, β -defensins, S100A15, RNase-7 and Histones (Buchau et al., 2007, Dorschner et al., 2001, Gallo and Hooper, 2012, Halverson et al., 2015, Simanski et al., 2010, Sorensen et al., 2006, Yang et al., 2017) and induces members of the β -defensin family under conditions of inflammation, infection and wound healing (Mangoni et al., 2016, Schneider et al., 2005) .

Several pivotal studies have provided insight into the host response during cutaneous wound repair (Campbell et al., 2013, Grice et al., 2010) yet relatively little is known about the skin

microbiota and whether they have detrimental or beneficial impacts on repair. Here, we demonstrate an association between the bacterial profile of non-infected human DFUs and healing outcome, correlating with upregulated expression of the PRR *NOD2*. Using both *NOD2* stimulated and *Defb14* null murine models we reveal new insights into the role of the innate defense response in controlling the skin microbiota during wound repair.

RESULTS

Human chronic wound microbiome is linked to healing outcome

Patients were recruited with chronic non-infected DFUs (Grade A1/B1, no infection or ischemia at the time of presentation). Total eubacterial diversity was profiled using 16S PCR-Density Gradient Gel Electrophoresis (16S PCR-DGGE) on DFU punch biopsy tissue collected at clinical presentation (week 0). Patients were then separated into two groups according to their time to heal over a period of 12 weeks; DFU healed ≤ 7 weeks ($n = 10$) versus non-healed ≥ 12 weeks ($n = 9$). Eubacterial DNA profiles (UPGMA dendrogram) at presentation (week 0) showed clear segregation between wounds that would heal versus those that would not (Figure 1a; wound closure at ≤ 7 weeks (green) versus ≥ 12 weeks (purple), $n = 19$). 16S rRNA Illumina high-throughput sequencing of a further set of DFU samples ($n = 25$) and non-metric multidimensional analysis (NMDS) showed no clear separation between the microbial profiles of the healed compared to the non-healed wounds (Figure 1b); however, non-healing wounds were associated with significantly reduced overall phylum diversity (Figure 1c). Phylum level relative abundance was consistent between healed and non-healed wounds (Fig 1d); however, interestingly genus level taxonomic classification of the wound microbiome revealed a significantly altered microbial community in healed versus non-healed wounds, including relative abundance variation within common skin-associated taxa such as *Staphylococcus* (23% in healed wounds versus 19% in non-healing wounds), *Anaerococcus* (3% in healed wounds

versus 10% in non-healing wounds) and *Coprococcus* (classified in other genera category, Figure 1e ($P \leq 0.05$)). The taxonomic information for all mapped reads at the genus level can be found in the supplementary material (Table S2). Finally, the overall presence of bacteria in wounds was assessed by direct Gram stain of DFU biopsy tissue which revealed no significant difference in bacterial numbers between the groups (Figure 1f-g). Collectively this data suggests that bacterial community diversity rather than overall bacterial burden correlates with DFU healing outcome.

NOD2 is upregulated in human chronic wounds that fail to heal

We next assessed whether PRR expression was altered as PRRs have been implicated in the skin microbiome regulation (Campbell et al., 2013, Dasu et al., 2010, Lai et al., 2009, Lin et al., 2012). Several TLRs trended towards increased expression in non-healing wounds (Figure 2a-e) but only the intracellular PRR *NOD2* was significantly increased ($P < 0.05$, Figure 2f). *NOD2* is implicated in barrier function, epithelial turnover and repair (Cruickshank et al., 2008) therefore we investigated *NOD2* function in keratinocytes. Keratinocyte scratch wound closure was significantly reduced following treatment with the *NOD2* ligand, MDP ($P < 0.05$, Figure 2g-h). Scratch closure was also inhibited by a range of TLR ligands (Figure S1a); however, TLR2 ligands did not affect closure. The addition of mitomycin C to inhibit proliferation (Figure 2h) showed no difference in migration between MDP treatment and control, implicating *NOD2* signalling in the proliferative component of scratch wound closure. qPCR confirmed that MDP treatment significantly increased keratinocyte mRNA expression of *NOD2* ($P < 0.05$, Figure 2i).

Experimental stimulation of the NOD2 pathway delays cutaneous wound healing

We next investigated the impact of NOD2 activation using C57BL/6 mice subcutaneously injected with MDP or vehicle control, prior to incisional wounding. MDP treatment upregulated *Nod2* mRNA in the wound (Figure S1b) and showed a trend for upregulation of the *Nod2* associated downstream signalling molecules *Rip2* but not *Tak1*, (Figure S1c-d). MDP treatment significantly delayed wound closure (Figure 3a) demonstrated by increased histological wound area ($P<0.001$, Figure 3b) and reduced re-epithelialization ($P<0.01$, Figure 3c). MDP-treated wounds had increased local wound recruitment of both neutrophils ($P<0.001$) and macrophages ($P<0.01$, Figure 3d-f) and we observed an extended keratinocyte activation response (extension of keratin 6 staining from the wound edge compared to control; $P<0.01$, Figure 3g-h). In line with these results, Ki67 staining in MDP treated wounds, demonstrated significantly increased wound edge proliferation in MDP-treated wounds (Figure 3i-j). Collectively, these results demonstrate that MDP-mediated activation of NOD2 significantly delays repair.

NOD2 stimulation induces an anti-microbial response in cutaneous wound healing

NOD2 has a known role in gut and lung epithelial AMP production specifically defensins (Rohrl et al., 2008, Tan et al., 2015). MDP treated wounds had significantly upregulated levels of *mBD3* ($P<0.05$) and *mBD14* ($P<0.05$) mRNA compared to control wounds (Figure 4a). Similarly, *in vitro*, MDP stimulated NHEKs significantly induced *hBD1*, *hBD2* (the human orthologue to mBD3) and particularly *hBD3* (the human orthologue to mBD14; $P<0.05$, Figure 4b). We further explored the effect of mBD14 on wound healing, focusing on the keratinocyte response. We used a mBD14 peptide (Reynolds et al., 2010), which we confirmed as biologically active as it inhibited *P. aeruginosa* growth (Figure S2a) and scratch-wounded primary mouse keratinocyte monolayers were treated with 1, 10 or 25 $\mu\text{g/ml}$ of mBD14 peptide. Keratinocyte migration was significantly decreased in a dose-dependent manner

($P<0.01$, Figure 4c-d). Importantly, cell viability was unaffected by the peptide as determined by examination of morphological features, suggesting that mBD14 directly influences epidermal migration. The sequence homology between mBD14 and hBD3 is approximately 69% (Hinrichsen et al., 2008, Rohrlet al., 2008), therefore we tested mBD14 peptide on human keratinocytes with similar results (Figure S2b). We also investigated the impact of hBD3 on keratinocyte function using hBD3 transfected cells; however, we saw no effect on keratinocyte scratch closure (Figure S2c).

β -defensin 14 null mice had delayed wound healing

To further clarify the role of mBD14 we investigated excisional wound healing in mice that lack BD14 (*Defb14^{-/-}*) and WT littermate controls. Histological analysis revealed delayed wound repair in *Defb14^{-/-}* mice (Figure 5a), with significantly increased wound area ($P<0.01$, Figure 5b) and delayed re-epithelialization ($P<0.05$, Figure 5c) at 3 days post-wounding. There was a significant reduction in neo-epidermal area although no difference in the distance contribution of keratin 6 expressing cells ($P<0.05$, Figure 5d-f). *Defb14^{-/-}* wounds had an extended epidermal proliferative response compared to control, with increased numbers of Ki67 expressing basal keratinocytes at the peri-wound edge ($P<0.05$, Figure 5g-h). Examination of the immune cells revealed no change in wound neutrophils (Figure 5i), but significantly increased macrophages suggesting altered immune response dynamics ($P<0.01$; Figure 5j). *Defb14^{-/-}* wounds had increased wound granulation tissue iNOS⁺ cells (associated with classically activated macrophages) at 3 days post-wounding ($P<0.01$, Figure 5k), and a concomitant trend towards a decrease in Arg1⁺ cells (expressed by alternatively activated macrophages) compared to controls (Figure 5l). Collectively, these data suggest an altered epidermal response and a highly pro-inflammatory local wound environment in the absence of β -defensin 14.

β -defensin 14 null mice have an altered wound bacterial profile

Chronic wounds had altered communities of bacteria compared with wounds that healed well and we had shown that mBD14 peptide inhibited the growth of *P. aeruginosa* (Figure S2a) therefore, we assessed bacterial abundance in *Defb14*^{-/-} mice. Total eubacterial abundance was significantly increased in *Defb14*^{-/-} mice compared to controls as revealed by Gram-staining ($P<0.01$, Figure 6a-b) and 16S qPCR ($P<0.05$, Figure 6c). qPCR analysis of common skin bacterial species revealed increased levels of *P. aeruginosa* ($P<0.01$) as well as *P. acnes* ($P<0.05$, Figure 6d-g) implicating BD14 in a bacterial dysbiosis that is detrimental to healing.

DISCUSSION

Human skin is colonized by a diverse array of bacteria and microbes that generally live in harmony with the host, yet overgrowth of commensal species or pathogen infection can negatively impact healing (Grice and Segre, 2012a, 2012b). While the precise relationship between the microbes and healing remains unclear, diabetic wounds are thought to be colonized by distinct microbiota compared to normally healing wounds including increased *Pseudomonas aeruginosa* (Grice et al., 2010, Hinojosa et al., 2016, Price et al., 2011). However, not all wounds fail to heal and it remains unclear whether an altered skin microbiota is associated with a predisposition to delayed healing. The data presented here suggest that in the absence of clinical infection, microbiome profiles (and associated host response) play an important role in determining subsequent healing outcome. Thus, bacteria present on our skin prior to injury could dictate how we heal.

In DFU patients, rather than the more "common" wound pathogens, we observed changes in genera abundance such as *Corynebacterium*, *Enterococcaceae*, and *Helcococcus* associated

1 with non-healing. We assessed the DFU microbiome at time of clinical presentation before the
2 outcome of healing was known. Previous and complimentary longitudinal analysis of DFU-
3 associated bacteria have linked poor healing to a more stable microbiome, whereas wounds
4 that healed well had a more dynamic microbiome that transitioned between community types
5 (Loesche et al., 2017). Similarly, our findings implicate a less diverse microbiome at the
6 initiation of healing, which may in turn impact upon the subsequent dynamics of the
7 microbiome during healing. It remains unclear whether such observations will be broadly
8 applicable to other wound types such as venous leg ulcers, decubitus ulcers and wounds that
9 fail to heal by secondary intention. Studies do, however, suggest that neither patient
10 demographics nor wound type exert major influence on the bacterial composition of the chronic
11 wound microbiome (Wolcott et al., 2016).

12
13 Several previous studies have shown that TLRs are differentially regulated when comparing
14 acute wounds to chronic wounds, while a number of PRRs, such as TLR3, are important for
15 wound chronicity (Campbell et al., 2013, Dasu et al., 2010, Lai et al., 2009, Lin et al., 2012).
16 By contrast, our study tested PRR levels in longitudinally evaluated healing versus non-healing
17 chronic wounds. In this context, the only PRR to show statistically significant alteration was
18 NOD2. As the expression of NOD2 can be upregulated in response to bacterial ligation, it is
19 plausible that the observed differential NOD2 levels in non-healing wounds may reflect a
20 response to the differential bacterial composition of the wound environment.

21
22 We further investigated the effect of experimentally activating NOD2 in a murine model, via
23 the ligand muramyl dipeptide (MDP). Here MDP treatment led to a significant delay in healing.
24 Studies have linked *NOD2* dysregulation to an altered innate immune response, susceptibility
25 to inflammation and delayed healing in acute wounds from elderly subjects (Hardman and

Ashcroft, 2008, Lesage et al., 2002). NOD2, but not TLR2, has an essential role during re-epithelialisation following murine cutaneous injury (Campbell et al., 2013), and in the murine gut NOD2 regulates epithelial turnover and immune cell recruitment (Bowcutt et al., 2014, Cruickshank et al., 2008). In the clinical setting, mutations in *NOD2* are linked to the rare inflammatory skin condition Blau syndrome and delayed wound healing (Kurokawa et al., 2003). Functional studies, have shown that both loss-of-function and gain-of-function mutations in NOD2 are associated with chronic inflammation (Kobayashi et al., 2005, Watanabe et al., 2004). This apparent dichotomy is thought to be because NOD2 can directly drive pro-inflammatory signals as well as inhibit other pathways such as the TLR2 mediated pathway of inflammation (Watanabe et al., 2004). Other research suggests that the ability of NOD2 to mediate a pro-inflammatory or anti-inflammatory effect is dependent upon the nature of accessory factors present, such as cytokines or bacterial products (Feerick and McKernan, 2017). In this context, both NOD2 overexpression in human chronic wounds and Nod2 stimulation in murine wounds is associated with delayed wound closure.

NOD2 has a well-characterized role in the recognition and clearance of intracellular bacteria through activation of the pro-inflammatory pathway and other host defense pathways including AMPs (Philpott et al., 2014). In addition to anti-microbial roles (Hinrichsen et al., 2008), AMPs have been shown to modulate cytokine production (e.g. IL-1 β , IL-22), keratinocyte migration and proliferation, and angiogenesis (Harder et al., 2013, Ong et al., 2002). MDP stimulation of NOD2 led to a significant upregulation of mBD3 and 14 (mouse orthologue of human hBD2 and 3) in keratinocytes *in vitro* and wounded skin *in vivo*. Dysregulation of AMPs in the skin may be an important factor in the host susceptibility to bacterial colonization and wound repair.

Specific loss of *Defb14* (mDB14) severely impaired multiple aspects of wound healing, with reduced re-epithelization, increased inflammation and a higher bacterial burden including *P. aeruginosa*, which we have previously shown to be detrimental to the healing response (Williams et al., 2017). These findings support previous observations that AMPs have diverse functions, including modulation of the innate immune system and altering TLR responsiveness (Beaumont et al., 2014, McGlasson et al., 2017, Semple et al., 2015, Wang et al., 2017). Some AMPS, such as cathelicidin, promote neutrophil recruitment and anti-microbial-activity and indeed *Defb14*^{-/-} mouse wounds displayed limited neutrophil recruitment, despite delayed healing and a higher bacterial burden (Beaumont et al., 2014, Choi et al., 2012, Mookherjee and Hancock, 2007). The role of BD14 in keratinocytes is particularly poorly understood. Here we showed that treatment of *in vitro* keratinocyte scratch assays with mBD14 impaired scratch closure, although it remains unclear whether this is a direct effect or the result of activating other keratinocyte pro-repair pathways, such as local cytokine production (Wang et al., 2017).

Collectively our work suggests that a greater knowledge of host microbial interactions is essential to understand wound healing progression. Bacterial ligands and anti-microbial factors are almost invariably multifactorial in function, conveying both beneficial and detrimental impacts on healing. Specifically, understanding the dynamics of host-microbial interactions will be key for better managing the treatment of patients with chronic wounds. In the future simple diagnostic tests to rapidly stratify healing potential based on wound bacterial composition will likely be coupled with bacteria-selective treatments and/or selective manipulation of the microbiome to promote healing.

MATERIALS & METHODS

Human chronic wounds

Local ethical committee approval was obtained for all human studies, with informed consent obtained in accordance with the Declaration of Helsinki. 25 wound biopsy patient samples (mixed sex, aged ≥ 40 years) with chronic DFUs (defined as distal to the medial and lateral malleoli, with a known duration ≥ 4 weeks, grade A1/B1, University of Texas ulcer classification, no infection or ischaemia) were obtained at the time of presentation (week 0). All patients received standard-of-care treatment, including regular debridement, non-antimicrobial dressing, and offloading. No local anaesthetic was used at any time during treatment. At week 0 wound biopsy samples were collected from the margin of DFUs prior to debridement using aseptic technique. Photographs of patient's wounds were taken weekly over 12 weeks to determine longitudinal healing outcome. DFUs were then separated into two groups, those who healed (full wound closure at ≤ 7 weeks; 10 patients) and those who failed to heal (wound not closed at 12 weeks; 9 patients) following current best practice treatment.

Generation of hBD3 expressing HaCaT cell line

A human Beta Defensin 3 stably over-expressing HaCaT cell line was constructed by transfecting cells with a plasmid containing hBD3 cloned into pcDNA3.1 (kind gift of Julia Dorin, University of Edinburgh). Lipofectamine 2000 (Life Technologies) was used for transfection as per manufacturer's guidelines. Stably transfected cells were selected for by addition of 500 μ g/ml G418 (Life Technologies). Overexpression of hBD3 in the stable cell line compared to control vector transfected line was confirmed by Real Time PCR, using TaqMan primer probe to the coding region of hBD3 (Applied Biosystems, assay ID Hs04194486_g1).

Cell culture and scratch migration assay

HaCaT cells (established human keratinocyte cell line) were cultured in DMEM plus 5% FBS. Normal human epidermal keratinocytes (NHEK) (PromoCell, Heidelberg, UK,) were cultured in Keratinocyte Growth Medium 2 (PromoCell, C-20011) plus supplements (PromoCell). Primary murine keratinocytes were isolated and cultured (Hager et al., 1999), with collagen IV-coated plates and CnT-PR medium (CELLnTEC, Bern, Switzerland). Confluent keratinocyte sheets seeded in 24-well plates were 'scratch wounded' and treated with 1 µg/ml MDP (Bachem, St Helens, UK) with or without 20 µg/µl mitomycin C (Sigma-Aldrich, Dorset, UK); 0-25 µg/ml mBD14; 1µg/ml Lipopolysaccharide (LPS); 1µg/ml Pam3-Cys; 10⁷ CFU *Staphylococcus aureus* (SA); or 1µg/ml Peptidoglycan (PGN), for 24, 48 or 96 hours. Images were captured on a Nikon Eclipse E600 microscope (Nikon, Surrey, UK) and a SPOT insight camera (Image solutions Inc, Lancashire, UK). Scratch closure was quantified using Image Pro Plus software (Media Cybernetics, Cambridge, UK) averaged from fifteen measurements per sample. Calculations for percent closure were based on epithelial scratch width after specified duration (D), in relation to width at time zero (T0) using the equation ((T0-D)/T0)100).

RNA isolation and reverse transcription-quantitative PCR (RT-qPCR)

Total host RNA was isolated using the Purelink RNA kit (Invitrogen™ by Life Technologies Ltd, Paisley, UK). cDNA was transcribed from 1 µg of RNA (Promega RT Kit, Hampshire, UK and AMVreverse transcriptase, Roche, West Sussex, UK) and qPCR performed using the SYBR® Green 1 Kit (Eurogentec, Hampshire, UK) and an iCycler iQ quantitative PCR thermal cycler (Bio-Rad, Hertfordshire, UK). The primer sequences for real-time qPCR are listed in Table S1.

DNA extraction from tissue samples and manipulation

All tissue samples were incubated in enzymatic lysis buffer (20 mM Tris at pH 8.0, 0.2 mM EDTA, 1.2% triton X-100) and lysozyme (20 mg/ml) for 30 min at 37°C. DNA was extracted using a Qiagen DNeasy™ blood and tissue kit (Qiagen, West Sussex, UK).

PCR amplification, purification and denaturing gradient gel electrophoresis (DGGE)

The V3 variable region of the 16S rRNA gene was amplified from purified DNA by PCR using GC-rich eubacterium-specific primers P3_GC-341F and 518R (see Table S1) (Walter et al., 2000) using a PTC-100 DNA Engine thermal cycler (Bio-Rad). Samples were purified using a Qiagen MinElute® purification kit (Qiagen). Polyacrylamide electrophoresis was performed using the D-CODE Universal Mutation Detection System (Bio-Rad). Denaturing gradient gels of 10% (wt/vol) acrylamide-bisacrylamide (37:1:5) were made as described previously (Walter et al., 2000). DGGE gel images were aligned and analyzed with BioNumerics software version 4.6 (Applied Maths, Sint-Martens-Latem, Belgium) and profiles used to produce an Unweighted Pair Group Method with Arithmetic Mean (UPGMA) dendrogram.

16S rRNA gene sequencing analysis

16S amplicon sequencing targeting the V3 and V4 variable region of the 16S rRNA gene (Table S1) was performed on the Illumina MiSeq platform. The raw amplicon data was processed using quantitative insights into microbial ecology (QIIME) version 1.9.0 (Caporaso et al., 2010), and R version 3.3.1 (Team, 2016). The NMDS plot was created using the isoMDS function in the ‘MASS’ package (Venables and Ripley, 2002) in R and statistical analysis performed using the ‘adonis’ function in the ‘vegan’ package in R. The Shannon Wiener Diversity Index was also calculated in R, using the ‘diversity’ function in the ‘vegan’ package (Okansen et al., 2016).

Hucker-Twort Gram Stain

The Hucker-Twort Gram stain was used to distinguish Gram-positive and Gram-negative bacteria in formalin-fixed tissue. Slides were imaged using a 3D-Histech Pannoramic-250 Flash Slide Scanner (3D Histech, Budapest, Hungary), using a 20x/0.25 Plan Apochromat objective (Zeiss, Oberkochen, Germany). All tissue was blinded before analysis. The sum of scores for relative amounts of Gram-positive and Gram-negative bacteria in the wound bed tissue was quantified based on CMPT (Clinical Microbiology Proficiency-Testing) guidelines (score 0 to 4+), zero (score 0), rare or scant (score 1+), few (score 2+), moderate (score 3+) and many, numerous or heavy (score 4+) with regard to the numbers of organisms present per oil immersion field (x100).

Animals and wounding

Following local ethics committee approval, all animal studies were conducted in accordance with UK Home Office regulations. Mice were housed in isolator cages with *ad libitum* food and water. Wild-type (WT) (C57BL/6J) mice were bred from WTxWT matings and *Defb14* null mice (C57BL/6J background) were bred from heterozygous matings and have been described previously (Navid et al., 2012). Eight week-old female WT mice were anaesthetized and injected subcutaneously with 10 µg MDP (MurNAc-L-Ala-D-isoGln) (Bachem, UK, G-1055) or vehicle (PBS), 24 hours and repeated 2 hours prior to wounding ($n = 10$ mice/group). Mice were anaesthetized and wounded following our established protocol (Ansell et al., 2014). Briefly, two equidistant 1 cm full-thickness incisional or 6 mm excisional wounds were made through both skin and panniculus carnosus muscle at the injection site and left to heal by secondary intention.

Histology and immunohistochemistry (IHC)

Histological sections were prepared from tissue fixed in 10% buffered formalin saline and embedded in paraffin. 5 μ M sections were stained with haematoxylin and eosin or subjected to IHC analysis using keratin 6, keratin 14 (Covance, Maidenhead, UK, PRB-169P and PRB-155P); anti-Ki67 (Abcam, Cambridge, UK, ab16667); anti-neutrophil (Thermo Scientific, Runcorn, UK, MA1-40038); anti-Mac-3 (BD Biosciences, Oxford, UK, 553322); NOS2 (Santa Cruz Biotechnology, Heidelberg, Germany, SC-651); and arginase-I (Santa Cruz Biotechnology, SC-18354). Primary antibodies were detected using the appropriate biotinylated secondary antibody followed by ABC-peroxidase reagent (Vector Laboratories, Peterborough, UK, PK-6104 or PK-6101) with NovaRed substrate (Vector Laboratories, SK-4800) and counterstained with haematoxylin. Images were captured using a Nikon Eclipse E600 microscope (Nikon) and a SPOT insight camera (Image solutions Inc). Total immune cell numbers (quantification is illustrated in figure S3), granulation tissue wound area and percentage re-epithelialization were quantified using Image Pro Plus software (Media Cybernetics).

Minimum Inhibitory Concentrations (MIC)

MICs were determined using the microdilution method (Moore et al., 2008). Briefly, an overnight culture of *Pseudomonas aeruginosa* (NCTC 10781) was diluted in sterile Mueller-Hinton broth (Oxoid, Basingstoke, UK) to an OD₆₀₀ of 0.5. The biologically active form of the mBD14 peptide (Reynolds et al., 2010), FLPKTLRKFFCRIRGGRCVNLNCLGKEEQIGRCSNSGRKCCRKKK (oxidized cysteines to form 3 disulfides) (Cambridge Peptides, Cambridge, UK), was serially diluted in inoculated media and incubated at 37°C for 24 hours with agitation. Growth was measured as light absorbance (495 nm) relative to un-inoculated and detected using a microtiter plate reader (Powerwave XS, Bio Tek Instruments, Potton, UK).

Statistical analysis

Normal distribution and statistical comparisons between groups were determined using Shapiro-Wilk test, Student's *t*-test (two tailed), one or two-way ANOVA with Tukey post hoc test where appropriate using GraphPad Prism 7 Version 7.01 (GraphPad Software, Inc. La Jolla, CA) with the exception of the analysis for 16S rRNA gene sequencing analysis. For all statistical tests, the variance between each group was determined and probability values of less than $P<0.05$ were considered statistically significant.

CONFLICT OF INTEREST

The authors state no conflict of interest.

ACKNOWLEDGEMENTS

The authors would like to thank Professor Andrew Boulton for providing chronic wound tissue, Professor Werner Muller for generous provision of *Defb14* null mice, and Dr Catherine Walker and Dr Sarah Forbes for valuable technical assistance with design of BD14 peptide. The Histology Facility equipment that was used in this study was purchased by the University of Manchester Strategic fund. Special thanks go to Peter Walker for his help with the histology. The Bioimaging Facility microscopes used in this study were purchased with grants from BBSRC, Wellcome and the University of Manchester Strategic Fund. Special thanks go to Roger Meadows for help with microscopy and image analysis. This research was supported by an AgeUK Senior Fellowship (M.J.H), MRC Centenary award (M.J.H and A.J.M) and the Medical Research Council (MRC) project grant G1000449 (M.J.H and S.C.). DD was funded by an MRC senior non-clinical fellowship (G1002046).

REFERENCES

- Ansell D. M., Campbell L., Thomason H. A., Brass A., Hardman M. J. A statistical analysis of murine incisional and excisional acute wound models. *Wound Repair Regen* 2014;22(2):281-7.
- Attinger C., Wolcott R. Clinically Addressing Biofilm in Chronic Wounds. *Adv Wound Care* 2012;1(3):127-32.
- Beaumont P. E., McHugh B., Gwyer Findlay E., Mackellar A., Mackenzie K. J., Gallo R. L., et al. Cathelicidin host defence peptide augments clearance of pulmonary *Pseudomonas aeruginosa* infection by its influence on neutrophil function in vivo. *PLoS One* 2014;9(6):e99029.
- Bowcutt R., Bramhall M., Logunova L., Wilson J., Booth C., Carding S. R., et al. A role for the pattern recognition receptor Nod2 in promoting recruitment of CD103+ dendritic cells to the colon in response to *Trichuris muris* infection. *Mucosal Immunol* 2014;7(5):1094-105.
- Buchau A. S., Hassan M., Kukova G., Lewerenz V., Kellermann S., Wurthner J. U., et al. S100A15, an antimicrobial protein of the skin: regulation by *E. coli* through Toll-like receptor 4. *J Invest Dermatol* 2007;127(11):2596-604.
- Campbell L., Williams H., Crompton R. A., Cruickshank S. M., Hardman M. J. Nod2 deficiency impairs inflammatory and epithelial aspects of the cutaneous wound-healing response. *J Pathol* 2013;229(1):121-31.
- Caporaso J. G., Kuczynski J., Stombaugh J., Bittinger K., Bushman F. D., Costello E. K., et al. QIIME allows analysis of high-throughput community sequencing data. *Nat Methods* 2010;7(5):335-6.
- Choi K. Y., Chow L. N., Mookherjee N. Cationic host defence peptides: multifaceted role in immune modulation and inflammation. *J Innate Immun* 2012;4(4):361-70.

1 Cruickshank S. M., Wakenshaw L., Cardone J., Howdle P. D., Murray P. J., Carding S. R.
2 Evidence for the involvement of NOD2 in regulating colonic epithelial cell growth and
3 survival. *World J Gastroenterol* 2008;14(38):5834-41.

4 Dasu M. R., Devaraj S., Park S., Jialal I. Increased toll-like receptor (TLR) activation and TLR
5 ligands in recently diagnosed type 2 diabetic subjects. *Diabetes Care* 2010;33(4):861-8.

6 Dorschner R. A., Pestonjamasp V. K., Tamakuwala S., Ohtake T., Rudisill J., Nizet V., et al.
7 Cutaneous injury induces the release of cathelicidin anti-microbial peptides active against
8 group A *Streptococcus*. *J Invest Dermatol* 2001;117(1):91-7.

9 Dutta P., Das S. Mammalian Antimicrobial Peptides: Promising Therapeutic Targets Against
10 Infection and Chronic Inflammation. *Curr Top Med Chem* 2016;16(1):99-129.

11 Eming S. A., Martin P., Tomic-Canic M. Wound repair and regeneration: mechanisms,
12 signaling, and translation. *Sci Transl Med* 2014;6(265):265sr6.

13 Feerick C. L., McKernan D. P. Understanding the regulation of pattern recognition receptors
14 in inflammatory diseases - a 'Nod' in the right direction. *Immunology* 2017;150(3):237-47.

15 Gallo R. L., Hooper L. V. Epithelial antimicrobial defence of the skin and intestine. *Nat Rev*
16 *Immunol* 2012;12(7):503-16.

17 Gambichler T., Skrygan M., Appelhans C., Tomi N. S., Reinacher-Schick A., Altmeyer P., et
18 al. Expression of human beta-defensins in patients with mycosis fungoides. *Arch Dermatol Res*
19 2007;299(4):221-4.

20 Glaser R., Harder J., Lange H., Bartels J., Christophers E., Schroder J. M. Antimicrobial
21 psoriasin (S100A7) protects human skin from *Escherichia coli* infection. *Nat Immunol*
22 2005;6(1):57-64.

23 Gottrup F. A specialized wound-healing center concept: importance of a multidisciplinary
24 department structure and surgical treatment facilities in the treatment of chronic wounds. *Am*
25 *J Surg* 2004;187(5A):38S-43S.

1 Grice E. A., Segre J. A. The human microbiome: our second genome. *Annu Rev Genomics*
2 *Hum Genet* 2012a;13:151-70.

3 Grice E. A., Segre J. A. Interaction of the microbiome with the innate immune response in
4 chronic wounds. *Adv Exp Med Biol* 2012b;946:55-68.

5 Grice E. A., Snitkin E. S., Yockey L. J., Bermudez D. M., Program N. C. S., Liechty K. W., et
6 al. Longitudinal shift in diabetic wound microbiota correlates with prolonged skin defense
7 response. *Proc Natl Acad Sci U S A* 2010;107(33):14799-804.

8 Hager B., Bickenbach J. R., Fleckman P. Long-term culture of murine epidermal keratinocytes.
9 *J Invest Dermatol* 1999;112(6):971-6.

10 Halverson T. W., Wilton M., Poon K. K., Petri B., Lewenza S. DNA is an antimicrobial
11 component of neutrophil extracellular traps. *PLoS Pathog* 2015;11(1):e1004593.

12 Harder J., Schroder J. M., Glaser R. The skin surface as antimicrobial barrier: present concepts
13 and future outlooks. *Exp Dermatol* 2013;22(1):1-5.

14 Hardman M. J., Ashcroft G. S. Estrogen, not intrinsic aging, is the major regulator of delayed
15 human wound healing in the elderly. *Genome Biol* 2008;9(5):R80.

16 Hinojosa C. A., Boyer-Duck E., Anaya-Ayala J. E., Nunez-Salgado A., Laparra-Escareno H.,
17 Torres-Machorro A., et al. Impact of the bacteriology of diabetic foot ulcers in limb loss.
18 *Wound Repair Regen* 2016;24(5):923-7.

19 Hinrichsen K., Podschun R., Schubert S., Schroder J. M., Harder J., Proksch E. Mouse beta-
20 defensin-14, an antimicrobial ortholog of human beta-defensin-3. *Antimicrob Agents*
21 *Chemother* 2008;52(5):1876-9.

22 James G. A., Swogger E., Wolcott R., Pulcini E., Secor P., Sestrich J., et al. Biofilms in chronic
23 wounds. *Wound Repair Regen* 2008;16(1):37-44.

1 Kobayashi K. S., Chamaillard M., Ogura Y., Henegariu O., Inohara N., Nunez G., et al. Nod2-
2 dependent regulation of innate and adaptive immunity in the intestinal tract. *Science*
3 2005;307(5710):731-4.

4 Kurokawa T., Kikuchi T., Ohta K., Imai H., Yoshimura N. Ocular manifestations in Blau
5 syndrome associated with a CARD15/Nod2 mutation. *Ophthalmology* 2003;110(10):2040-4.

6 Lai Y., Di Nardo A., Nakatsuji T., Leichtle A., Yang Y., Cogen A. L., et al. Commensal
7 bacteria regulate Toll-like receptor 3-dependent inflammation after skin injury. *Nat Med*
8 2009;15(12):1377-82.

9 Lesage S., Zouali H., Cezard J. P., Colombel J. F., Belaiche J., Almer S., et al. CARD15/NOD2
10 mutational analysis and genotype-phenotype correlation in 612 patients with inflammatory
11 bowel disease. *Am J Hum Genet* 2002;70(4):845-57.

12 Lin Q., Wang L., Lin Y., Liu X., Ren X., Wen S., et al. Toll-like receptor 3 ligand
13 polyinosinic:polycytidylic acid promotes wound healing in human and murine skin. *J Invest*
14 *Dermatol* 2012;132(8):2085-92.

15 Lipsky B. A., Peters E. J., Berendt A. R., Senneville E., Bakker K., Embil J. M., et al. Specific
16 guidelines for the treatment of diabetic foot infections 2011. *Diabetes Metab Res Rev* 2012;28
17 Suppl 1:234-5.

18 Loesche M., Gardner S. E., Kalan L., Horwinski J., Zheng Q., Hodgkinson B. P., et al. Temporal
19 Stability in Chronic Wound Microbiota Is Associated With Poor Healing. *J Invest Dermatol*
20 2017;137(1):237-44.

21 Mancl K. A., Kirsner R. S., Ajdic D. Wound biofilms: lessons learned from oral biofilms.
22 *Wound Repair Regen* 2013;21(3):352-62.

23 Mangoni M. L., McDermott A. M., Zasloff M. Antimicrobial peptides and wound healing:
24 biological and therapeutic considerations. *Exp Dermatol* 2016;25(3):167-73.

1 McGlasson S. L., Semple F., MacPherson H., Gray M., Davidson D. J., Dorin J. R. Human
2 beta-defensin 3 increases the TLR9-dependent response to bacterial DNA. *Eur J Immunol*
3 2017;47(4):658-64.

4 Misisic A. M., Gardner S. E., Grice E. A. The Wound Microbiome: Modern Approaches to
5 Examining the Role of Microorganisms in Impaired Chronic Wound Healing. *Adv Wound*
6 *Care (New Rochelle)* 2014;3(7):502-10.

7 Mookherjee N., Hancock R. E. Cationic host defence peptides: innate immune regulatory
8 peptides as a novel approach for treating infections. *Cell Mol Life Sci* 2007;64(7-8):922-33.

9 Moore L. E., Ledder R. G., Gilbert P., McBain A. J. In vitro study of the effect of cationic
10 biocides on bacterial population dynamics and susceptibility. *Appl Environ Microbiol*
11 2008;74(15):4825-34.

12 Navid F., Boniotto M., Walker C., Ahrens K., Proksch E., Sparwasser T., et al. Induction of
13 regulatory T cells by a murine beta-defensin. *J Immunol* 2012;188(2):735-43.

14 Okansen J. F., Blanchet G., Friendly M., Kindt R., Legendre P., McGlinn D., et al. vegan:
15 Community Ecology Package, <https://CRAN.R-project.org/package=vegan>; 2016 [Accessed
16 January 17 2017].

17 Ong P. Y., Ohtake T., Brandt C., Strickland I., Boguniewicz M., Ganz T., et al. Endogenous
18 antimicrobial peptides and skin infections in atopic dermatitis. *N Engl J Med*
19 2002;347(15):1151-60.

20 Papanas N., Mani R. Advances in infections and wound healing for the diabetic foot: the die is
21 cast. *Int J Low Extrem Wounds* 2013;12(2):83-6.

22 Philpott D. J., Sorbara M. T., Robertson S. J., Croitoru K., Girardin S. E. NOD proteins:
23 regulators of inflammation in health and disease. *Nat Rev Immunol* 2014;14(1):9-23.

1 Price L. B., Liu C. M., Frankel Y. M., Melendez J. H., Aziz M., Buchhagen J., et al. Macroscale
2 spatial variation in chronic wound microbiota: a cross-sectional study. *Wound Repair Regen*
3 2011;19(1):80-8.

4 Reynolds N. L., De Cecco M., Taylor K., Stanton C., Kilanowski F., Kalapothakis J., et al.
5 Peptide fragments of a beta-defensin derivative with potent bactericidal activity. *Antimicrob*
6 *Agents Chemother* 2010;54(5):1922-9.

7 Rhoads D. D., Cox S. B., Rees E. J., Sun Y., Wolcott R. D. Clinical identification of bacteria
8 in human chronic wound infections: culturing vs. 16S ribosomal DNA sequencing. *BMC Infect*
9 *Dis* 2012;12:321.

10 Rohrl J., Yang D., Oppenheim J. J., Hehlhans T. Identification and Biological Characterization
11 of Mouse beta-defensin 14, the orthologue of human beta-defensin 3. *J Biol Chem*
12 2008;283(9):5414-9.

13 Schneider J. J., Unholzer A., Schaller M., Schafer-Korting M., Korting H. C. Human defensins.
14 *J Mol Med (Berl)* 2005;83(8):587-95.

15 Semple F., MacPherson H., Webb S., Kilanowski F., Lettice L., McGlasson S. L., et al. Human
16 beta-Defensin 3 Exacerbates MDA5 but Suppresses TLR3 Responses to the Viral Molecular
17 Pattern Mimic Polyinosinic:Polycytidylic Acid. *PLoS Genet* 2015;11(12):e1005673.

18 Simanski M., Dressel S., Glaser R., Harder J. RNase 7 protects healthy skin from
19 *Staphylococcus aureus* colonization. *J Invest Dermatol* 2010;130(12):2836-8.

20 Sorensen O. E., Thapa D. R., Roupe K. M., Valore E. V., Sjobring U., Roberts A. A., et al.
21 Injury-induced innate immune response in human skin mediated by transactivation of the
22 epidermal growth factor receptor. *J Clin Invest* 2006;116(7):1878-85.

23 Tan G., Zeng B., Zhi F. C. Regulation of human enteric alpha-defensins by NOD2 in the Paneth
24 cell lineage. *Eur J Cell Biol* 2015;94(1):60-6.

25 Team R. C. 2016, <https://www.R-project.org>; 2016 [accessed 3rd January 2017].

Venables W. N., Ripley B. D. Modern Applied Statistics with S. 4th ed. New York: Springer, 2002.

Walter J., Tannock G. W., Tilsala-Timisjarvi A., Rodtong S., Loach D. M., Munro K., et al. Detection and identification of gastrointestinal *Lactobacillus* species by using denaturing gradient gel electrophoresis and species-specific PCR primers. *Appl Environ Microbiol* 2000;66(1):297-303.

Wang B., McHugh B. J., Qureshi A., Campopiano D. J., Clarke D. J., Fitzgerald J. R., et al. IL-1 β -Induced Protection of Keratinocytes against *Staphylococcus aureus*-Secreted Proteases Is Mediated by Human beta-Defensin 2. *J Invest Dermatol* 2017;137(1):95-105.

Watanabe T., Kitani A., Murray P. J., Strober W. NOD2 is a negative regulator of Toll-like receptor 2-mediated T helper type 1 responses. *Nat Immunol* 2004;5(8):800-8.

Williams H., Crompton R. A., Thomason H. A., Campbell L., Singh G., McBain A. J., et al. Cutaneous Nod2 Expression Regulates the Skin Microbiome and Wound Healing in a Murine Model. *J Invest Dermatol* 2017;137(11):2427-36.

Wolcott R. D., Hanson J. D., Rees E. J., Koenig L. D., Phillips C. D., Wolcott R. A., et al. Analysis of the chronic wound microbiota of 2,963 patients by 16S rDNA pyrosequencing. *Wound Repair Regen* 2016;24(1):163-74.

Yang B., Suwanpradid J., Sanchez-Lagunes R., Choi H. W., Hoang P., Wang D., et al. IL-27 Facilitates Skin Wound Healing through Induction of Epidermal Proliferation and Host Defense. *J Invest Dermatol* 2017;137(5):1166-75.

Zanger P. *Staphylococcus aureus* positive skin infections and international travel. *Wien Klin Wochenschr* 2010;122 Suppl 1:31-3.

FIGURE LEGENDS

Figure 1. The microbiome profile of human DFUs is an indicator of healing outcome. DFU samples were collected at baseline and their wound microbial communities sequenced by 16S

PCR-DGGE or 16S RNA Illumina high-throughput sequencing. Longitudinal healing was measured over the subsequent 12 weeks to define healing outcome. (a) UPGMA dendrogram of DFU DGGE fingerprints for healed (green) and non-healed (purple) wound tissue revealed clustering based on time to heal, $\geq 60\%$ intrapersonal variation versus $\leq 30\%$ interpersonal variation. (b) NMDS plot showing differences in clustering of microbial communities from 16S RNA Illumina high-throughput sequencing and (c) diversity which was calculated using Shannon Weiner. (d-e) Taxonomic classification of the skin microbiome, showing proportion of bacteria, in each treatment group, at the phylum level and genus level. Individual taxa with abundances too low to visualise clearly and unassigned reads are grouped into the ‘other’ category, comprised of 12 additional phyla plus unassigned reads at the phylum level, and 225 additional genera plus unassigned reads at the genus level. (f) Representative Gram stained histological sections and (g) quantification of numbers of bacteria per field of view. All data are representative of two independent experiments, with $n = 19$ patients for (a) and $n = 25$ for (b-g). * $P < 0.05$. P values were determined by one-way ANOVA (b-c); two-way ANOVA (d-e) with Tukey post hoc test or by a paired, two-tailed Student’s t -test (g). Mean + s.e.m. Scale bar = 20 μm (f).

Figure 2. Altered PRR expression in non-healing human DFUs. DFU samples were collected at baseline, with longitudinal healing measured over the subsequent 12 weeks. RT-qPCR profiling of (a-e) *TLR* members and (f) *NOD2* in patient wound samples collected at first visit with the patients subsequently categorized into either the healed wound group or the non-healed wound group. (g) Representative crystal-violet stained human keratinocyte scratch wounds stimulated with 1 $\mu\text{g/ml}$ MDP or control for 24 hours (dashed white line indicates initial scratch width; green line illustrates epidermal sheet edge measured) and (h) quantification of NHEK scratch closure in the presence or absence of mitomycin C. (i) *NOD2*

mRNA analyzed by qPCR. All data are representative of two-three independent experiments, with $n = 19$ patients in total (a-f), and $n = 7-8$ per treatment (g-i). * $P < 0.05$. P values were determined by a non-parametric permutational multivariate analysis of variance in a, or paired, two-tailed Student's t -test (b-i). Mean + s.e.m. Scale bar = 300 μm (g).

Figure 3. Stimulation of the *Nod2* pathway significantly delays murine cutaneous wound

healing. (a) Representative IHC (keratin 14) of control or MDP injected incisional wounds (day 3), arrows denote wound margins. (b) Analysis of histological wound area and (c) re-epithelialization. (d) Representative IHC of neutrophil and macrophages in control or MDP injected wounds at 3 days post-wounding, and quantification of (e) neutrophils and (f) macrophages (illustrated method figure S3). (g) Analysis of the distance contribution from the wound edge of keratin 6 expressing epidermal keratinocytes at 3 days post-wounding and (h) representative, keratin 6-stained images of control and MDP injected wounds at 3 days post-wounding; arrows indicate the cessation of keratin 6 expression. (i) Quantification of the percent of basal keratinocytes expressing proliferation marker Ki67. Wound edge = 0-500 μm from the wound and per-wound edge = 500-1000 μm from the wound. (j) Representative Ki67 staining, denoting location of wound and peri-wound edge. All data are representative of two-three independent experiments with $n = 6$ mice/group. *** $P < 0.001$, ** $P < 0.01$, * $P < 0.05$. P values were determined by paired, two-tailed Student's t -test. Mean + s.e.m. Scale bar = 200 μm (a, d), 50 μm (h,j).

Figure 4. *Nod2* stimulation alters defensin profile. qPCR analysis of cutaneous mBD1, 3 and

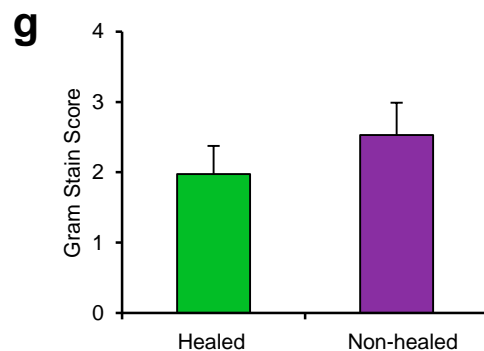
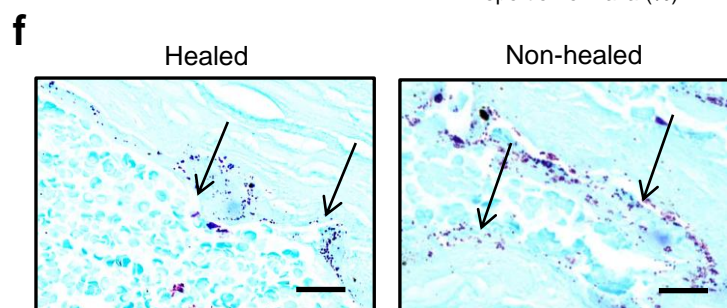
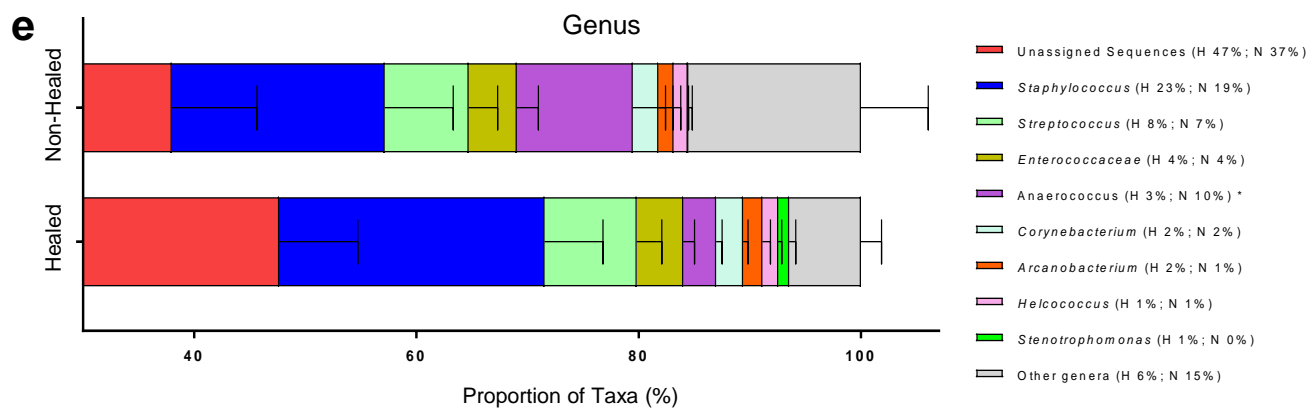
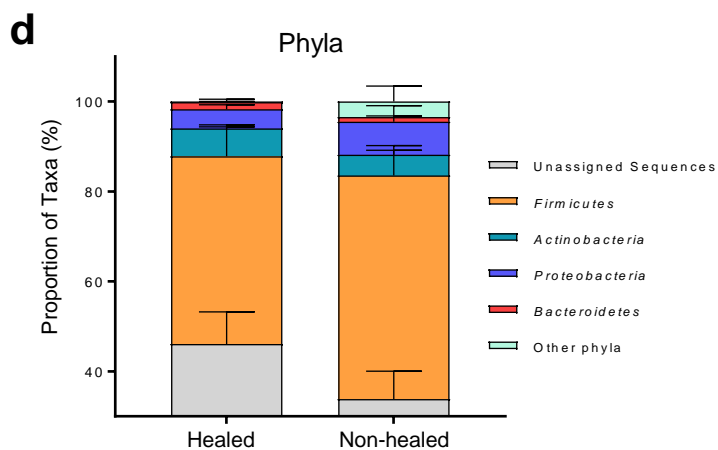
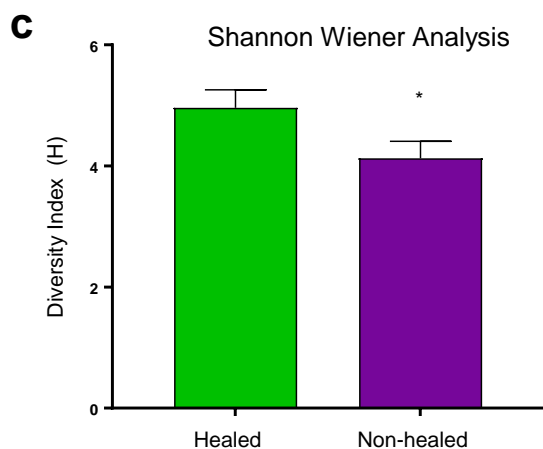
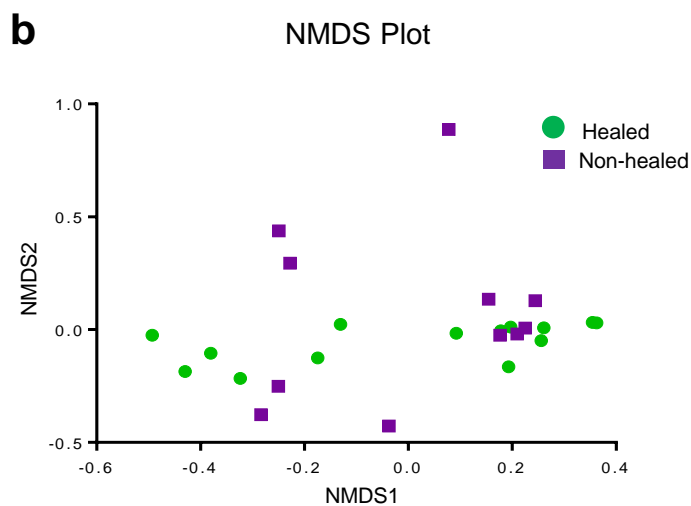
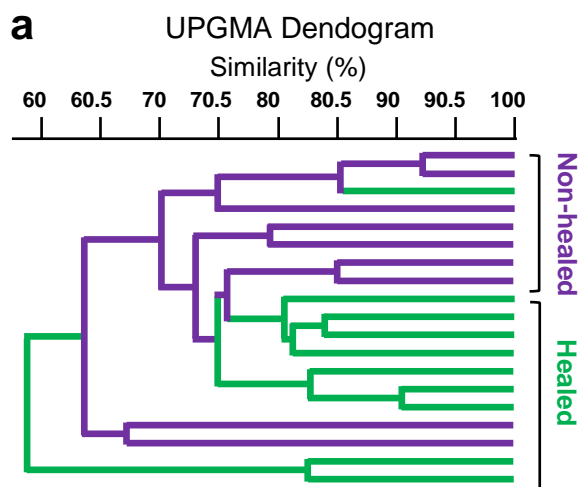
14 or hBD1, 2 and 3 in control versus 1 $\mu\text{g/ml}$ MDP treated (a) wounds or (b) NHEKs. (c) Primary mouse keratinocyte monolayers were scratched and treated with 1, 10 or 25 $\mu\text{g/ml}$ of mBD14 peptide and their closure assessed after 96 hours (dashed white line indicates initial

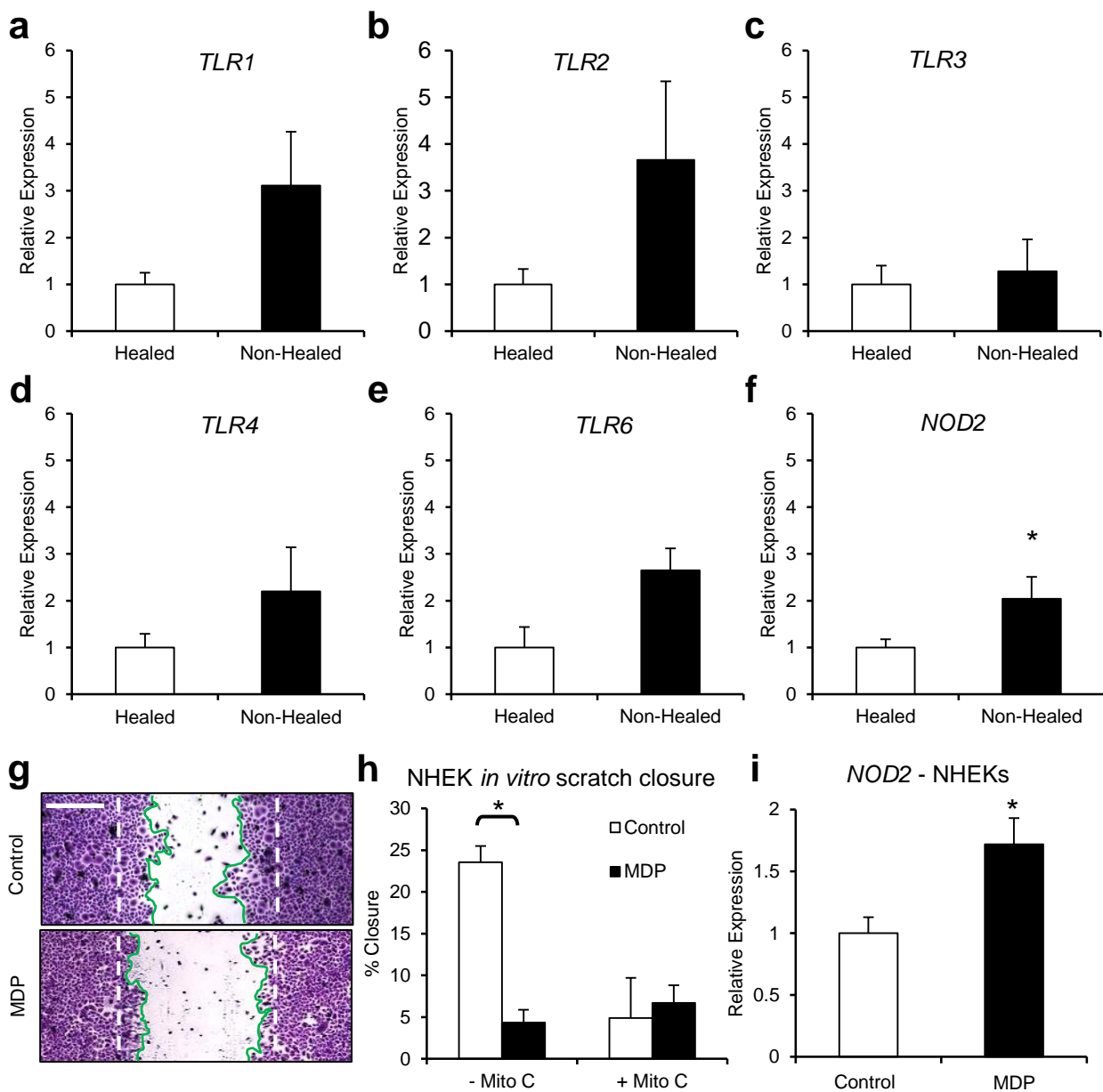
scratch width; green line illustrates epidermal sheet edge measured) (d). All data are representative of two-three independent experiments with $n = 6$ mice/group (a), and $n = 7-8$ wells/dose (b-d). *** $P < 0.001$, * $P < 0.05$. P values were determined by paired, two-tailed Student's t -test or one-way ANOVA for more than 2 groups. Mean + s.e.m..

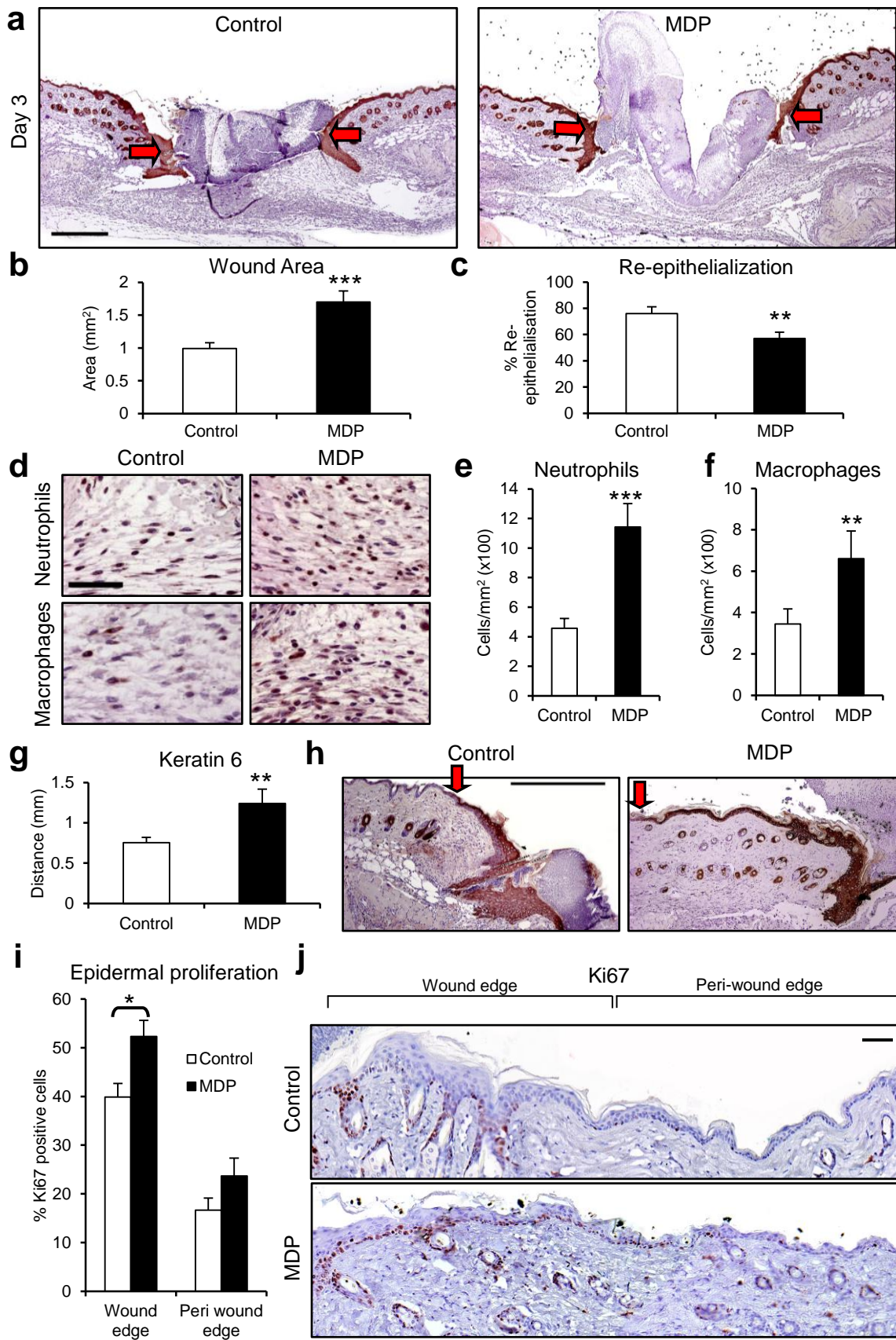
Figure 5. Delayed healing in *Defb14*-deficient mice. *Defb14*^{-/-} mice and littermate controls were excisionally wounded and analyzed three days post-wounding. (a) Representative hematoxylin and eosin stained sections of *Defb14*^{-/-} excisional wounds (day 3), arrows indicate wound margins. Analysis of histological wound area (b), and re-epithelialization (c) at day 3 post-wounding. Analysis of the distance contribution from the wound edge (d) and neo-epidermal area (e) of keratin 6 expressing epidermal keratinocytes, illustrated in representative images of WT and *Defb14*^{-/-} wounds at 3 days post-wounding (f); dashed outline indicates neo-epidermal area. (g) Quantification of the percent of basal keratinocytes expressing proliferation marker Ki67. Wound edge = 0-500 μ m from the wound and per-wound edge = 500-1000 μ m from the wound. (j) Representative Ki67 staining, denoting location of wound and peri-wound edge. IHC quantification of (i) neutrophils and (j) macrophages. Further characterisation of macrophage polarisation looked at the proportion of (k) iNOS⁺ or (l) Arg1⁺ macrophages (illustrated method figure S3). All data are representative of two independent experiments with $n = 5-6$ mice/group. ** $P < 0.01$, * $P < 0.05$. P values were determined by paired, two-tailed Student's t -test. Mean + s.e.m. Scale bar = 200 μ m (a); 100 μ m (f); 50 μ m (h, i-l).

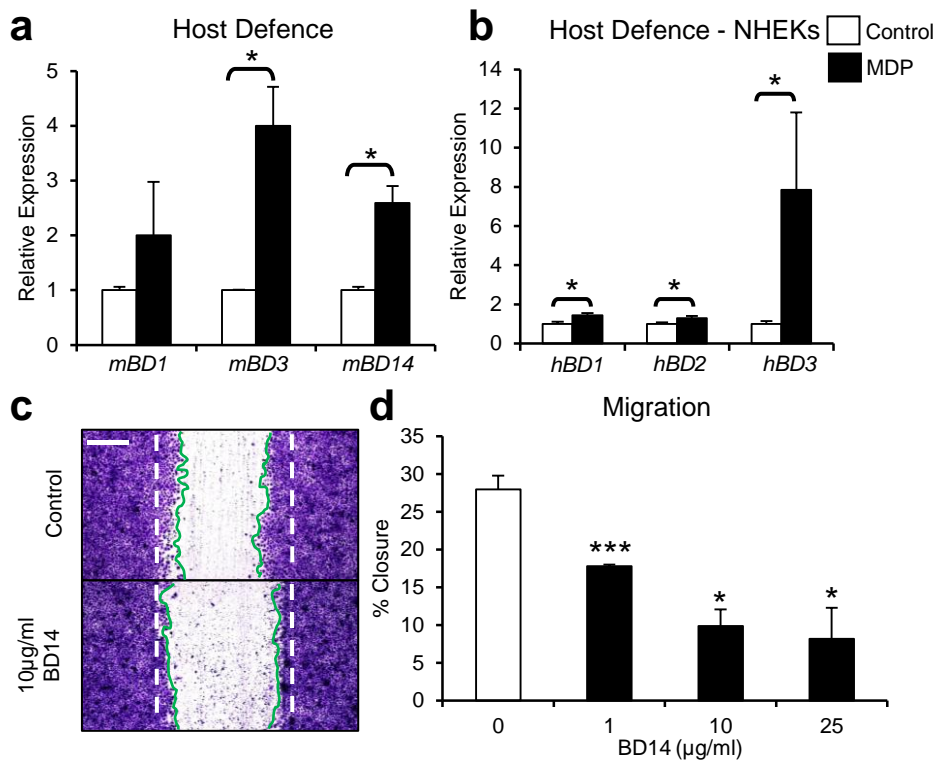
Figure 6. Bacterial dysbiosis in *Defb14*-deficient mice. (a) Gram-stain of representative histological sections and (b) quantification reveals altered bacterial burden in *Defb14*^{-/-} day 3 wounds compared to control. (c) This is confirmed through RT-qPCR (eubacterial 16S) of total bacterial abundance which demonstrates a significant increase compared to WT littermate

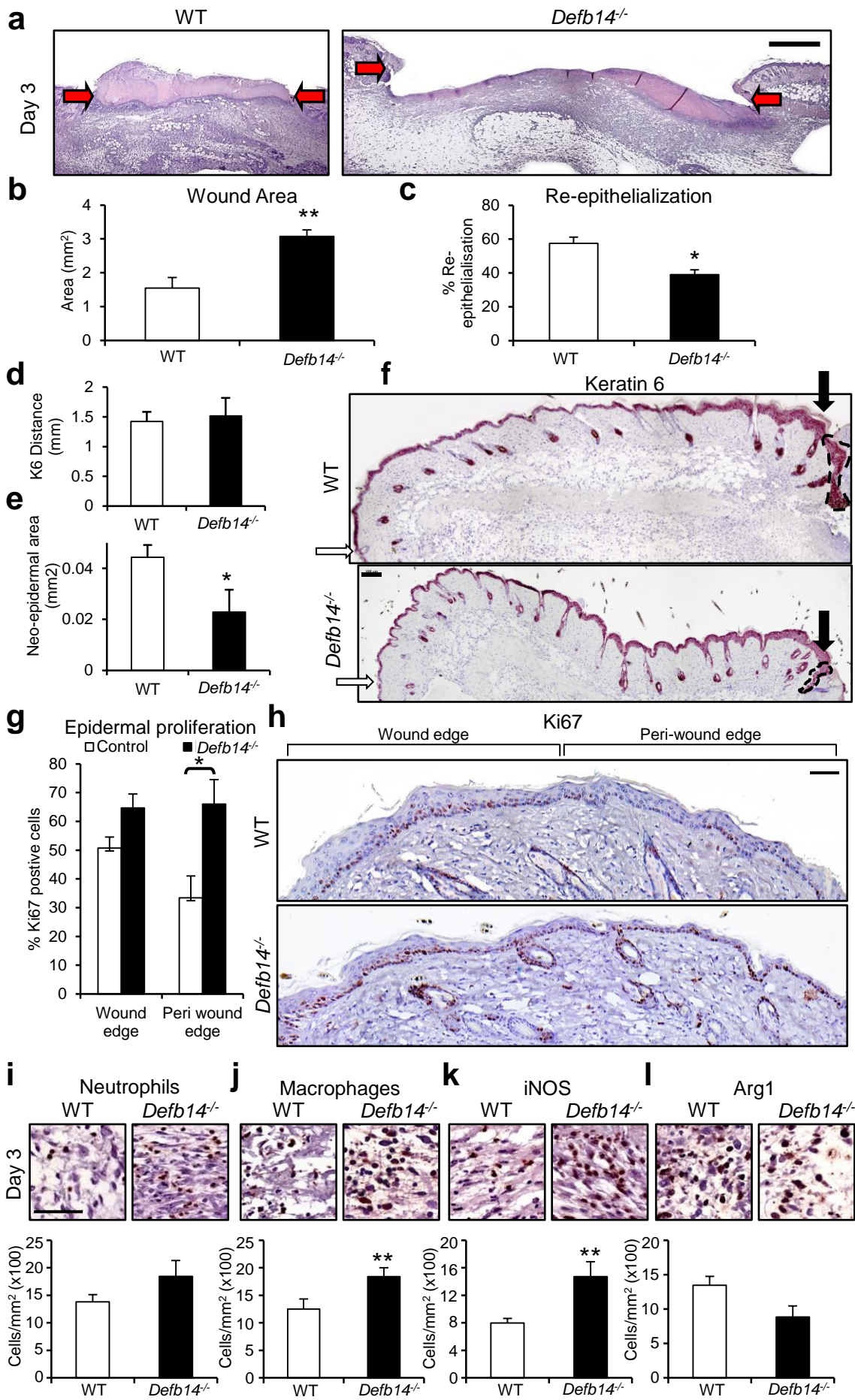
controls. These differences are associated with a significant increase of (d) *P. aeruginosa*, and
(e) *P. acnes* as revealed by RT species-specific qPCR. All data are representative of two
independent experiments with $n = 5-6$ mice/group. ** $P < 0.01$, * $P < 0.05$. P values were
determined by paired, two-tailed Student's t -test. Mean + s.e.m. Scale bar = 20 μm (a).

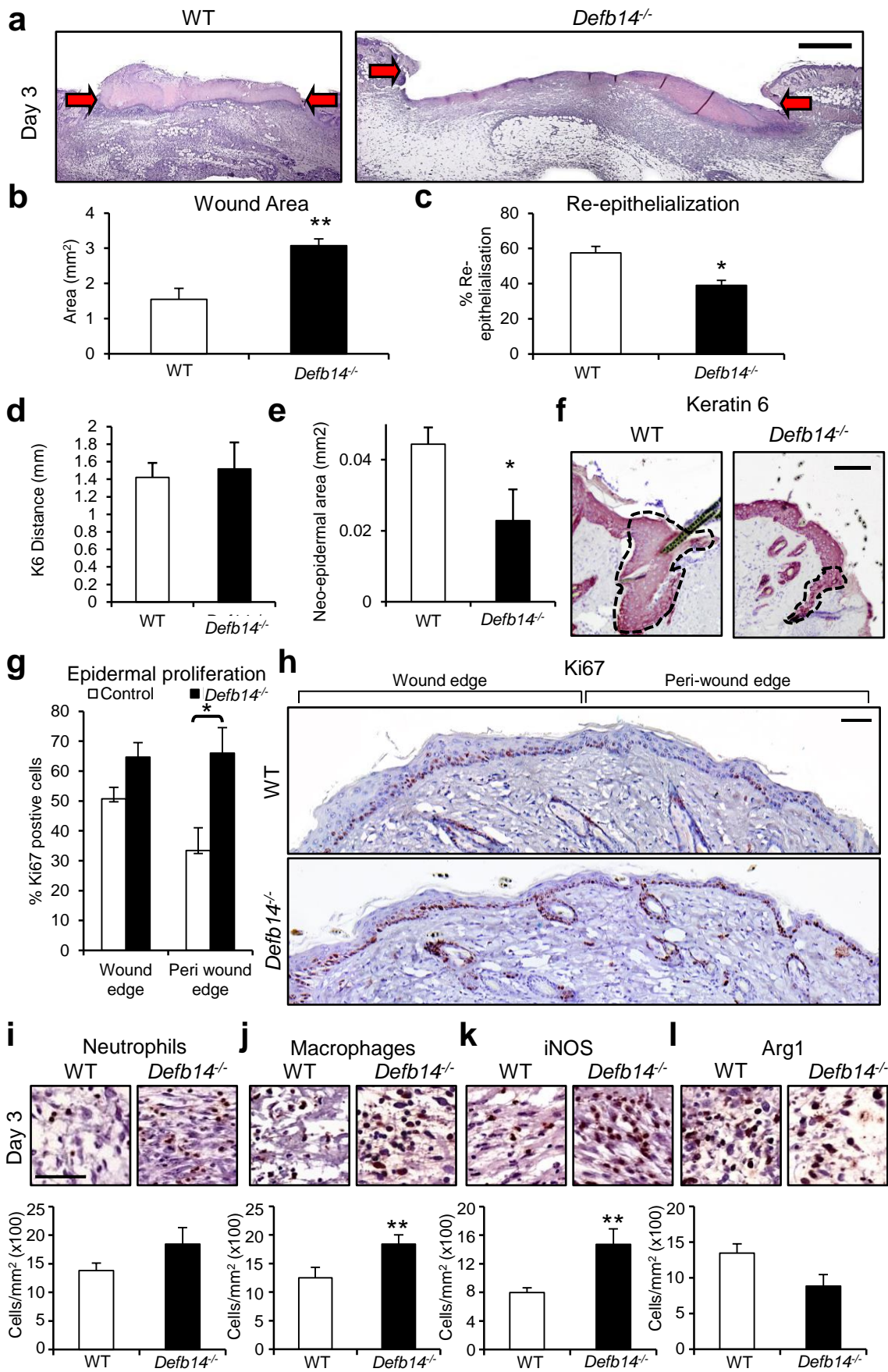


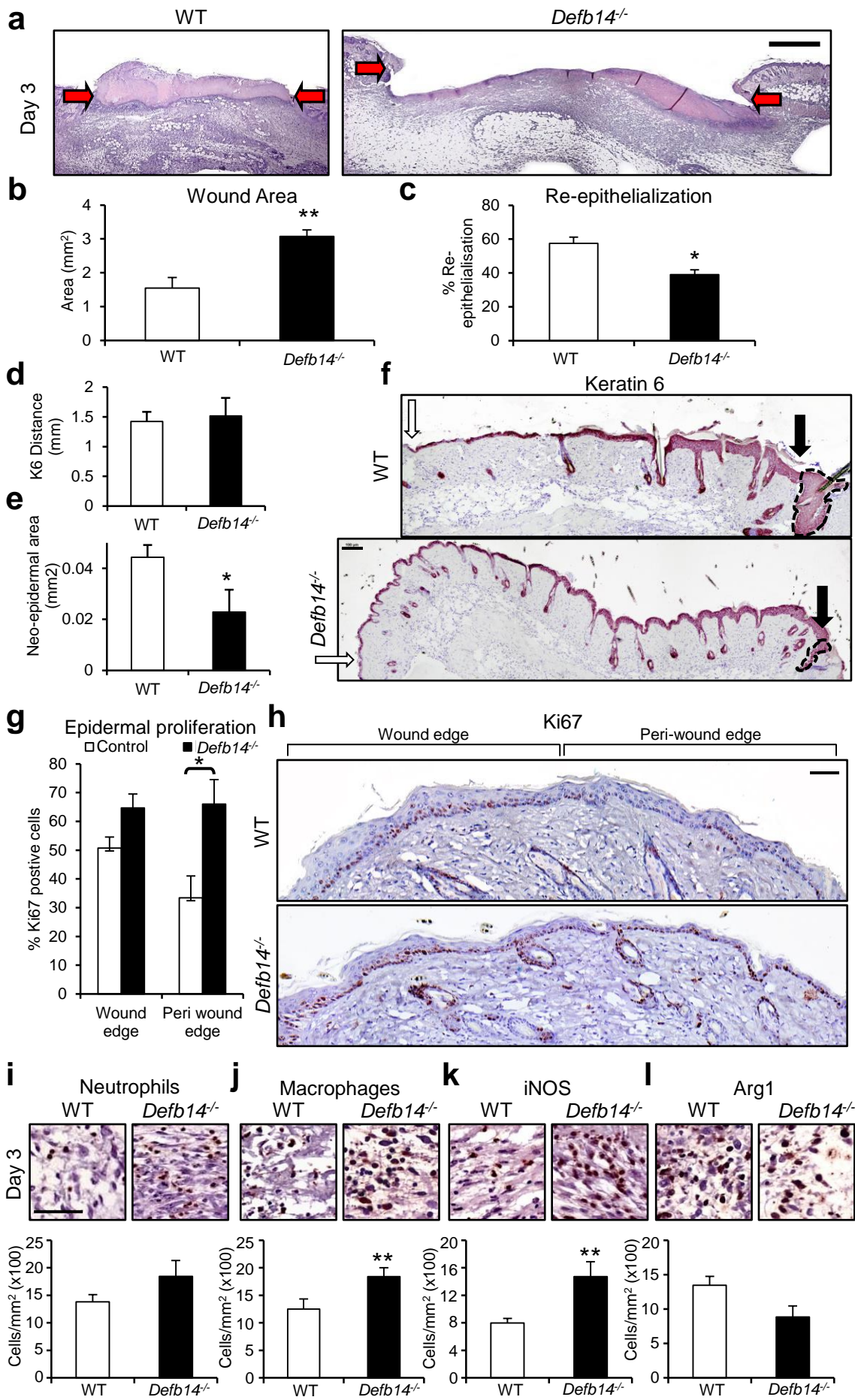


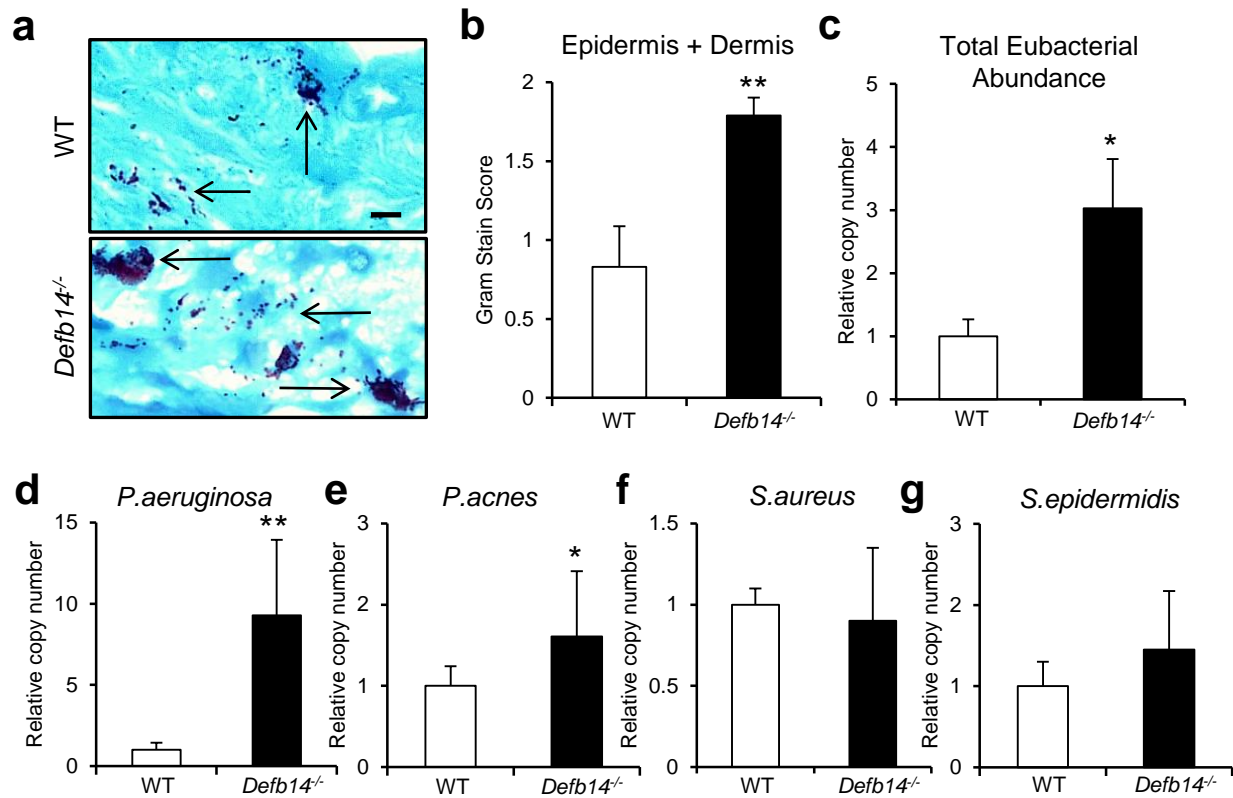




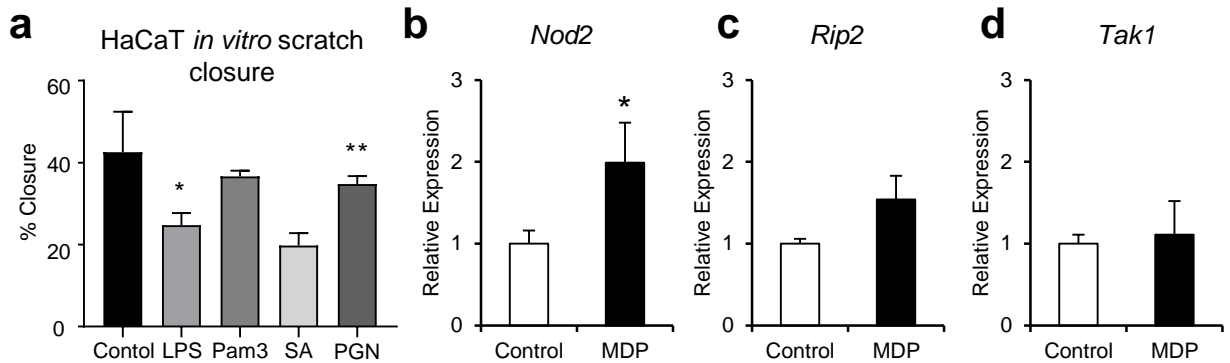






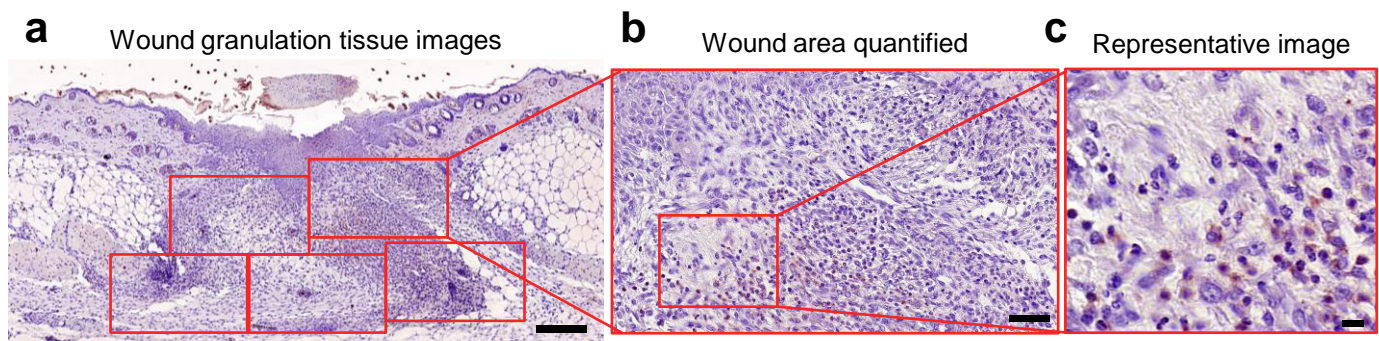


SUPPLEMENTARY MATERIAL

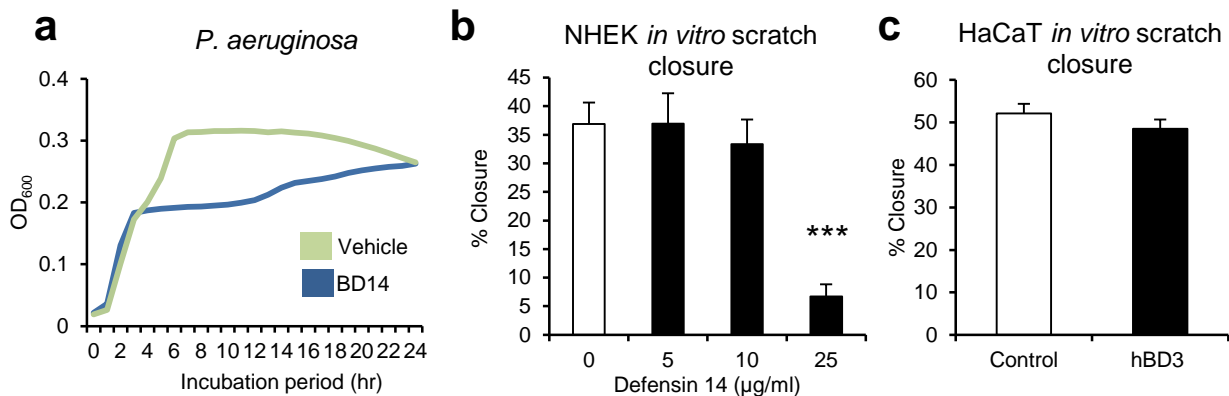


Supplementary Figure S1: Selective PRR activation in wound healing models.

(a) PRR ligand treated HaCaT wound closure, 24hrs post scratch. Bacterial ligands = 1 μ g/ml Lipopolysaccharide (LPS); 1 μ g/ml Pam3-Cys; 10⁷ CFU *Staphylococcus aureus* (SA); 1 μ g/ml Peptidoglycan (PGN). (b-d) Expression of *Nod2* (mRNA) and associated signalling components (*Rip2* and *Tak1*) is significantly increased in MDP stimulated wounds compared to control at 3 days post-wounding. All data are representative of two-three independent experiments with $n = 6$ mice/group. ** $P < 0.01$, * $P < 0.05$. P values were determined by paired two-tailed Student's t -test. Mean + s.e.m.



Supplementary Figure S2: Immune cell quantification method. (a) Approximately 5 x20 images of immune cell immunohistochemical staining are captured to encompass the wound granulation tissue area. Scale bar = 200µm. (b) Red/brown positively stained cells are counted using the colour selection tool and area of granulation tissue measured (excluding epidermis, fat and muscle) using Image Pro software. Scale bar = 50µm. (c) Representative images are displayed at higher magnification enabling clear visualisation of cell staining. Scale bar = 10µm.



Supplementary Figure S3: mBD14 peptide inhibits bacterial growth and keratinocyte migration *in vitro*. (a) mBD14 peptide was confirmed as biologically active using the MIC assay to assess *P. aeruginosa* growth. Data shows growth assay of *Pseudomonas aeruginosa* in the presence or absence of mBD14 peptide (25 μg/ml) (b) Primary human keratinocyte monolayers were scratched and treated with 1, 10 or 25 μg/ml of mBD14 peptide and their migration assessed after 48 hours. (c) hBD3 transfected and plasmid control HaCaT cell monolayers were scratched and closure assessed after 24hrs. * $P < 0.05$ All data are representative of two-three independent experiments with $n = 3-4$ /group.